AGU ADVANCING EARTH AND SPACE SCIENCES

Geophysical Research Letters

RESEARCH LETTER
10.1029/2023GL105674

Heterogeneous Crustal Structure of the Hikurangi Plateau Revealed by SHIRE Seismic Data: Origin and Implications for Plate Boundary Tectonics

Dan Bassett[1], Gou Fujie[2], Shuichi Kodaira[2], Ryuta Arai[2], Yojiro Yamamoto[2], Stuart Henrys[1], Dan Barker[1], Andrew Gase[3], Harm van Avendonk[3], Nathan Bangs[3], Hannu Seebeck[1], Brook Tozer[1], Katie Jacobs[1], Thomas Luckie[4], David Okaya[4], and Kimi Mochizuki[5]

[1]GNS Science, Lower Hutt, New Zealand, [2]Japan Agency for Marine-Earth Science and Technology, Yokohama, Japan, [3]Jackson School of Geosciences, Institute for Geophysics, University of Texas at Austin, Austin, TX, USA, [4]University of Southern California, Los Angeles, CA, USA, [5]Earthquake Research Institute (ERI), University of Tokyo, Tokyo, Japan

Abstract Marine multichannel and wide-angle seismic data constrain the distribution of seamounts, sediment cover sequence and crustal structure along a 460 km margin-parallel transect of the Hikurangi Plateau. Seismic reflection data reveals five seamount up-to 4.5 km high and 35–75 km wide, with heterogeneous internal velocity structure. Sediment cover decreases south-to-north from ~4.5 km to ~1–2 km. The Hikurangi Plateau crust (V_p 5.5–7.5 km/s) is 11 ± 1 km thick in the south, but thins by 3–4 km further north (~7–8 km). Gravity models constructed along two seismic lines show the reduction in crustal thickness persists further east, coinciding with a bathymetric scarp. Gravity data suggest the transition in crustal thickness may reflect spatial variability in deformation and lithospheric extension associated with plateau breakup. Variability in the thickness of subducting crust may contribute to differences in megathrust geometry, upper-plate stress state and high-rates of contraction and uplift along the southern Hikurangi margin.

Plain Language Summary The thickness of crust arriving at subduction zones exerts a major influence on the configuration, structure, and distribution of stresses at plate boundaries. A region of thickened oceanic crust, the Hikurangi Plateau, is subducting beneath the North Island of New Zealand. To understand the structure of this Plateau, we analyze seismic data along a 460 km long transect, which reveals five large seamounts, and a 3–4 km reduction crustal thickness between the southern and northern areas of the Plateau. Gravity data show this difference is persistent across the plateau and reveal structures suggesting the crust may have thinned when the Hikurangi plateau separated from a second plateau (Manihiki), which is thought to have formed at the same time. We propose that the subduction of thicker crustal along the southern Hikurangi margin may contribute to the shallow angle of the subducting plate, and high rates of uplift and deformation in the overthrusting plate.

Key Points:

- Crustal thickness of the Hikurangi Plateau reduces by ~30% between the southern (10–11 km) and northern (7–8 km) Plateau
- Coincident contrasts in plateau fabric may attribute the thickness contrast to rifting from the Manihiki Plateau
- Thickness contrasts may impact the geometry of the subducting plate and rates of upper-plate compression and uplift along the Hikurangi margin

Supporting Information:

Supporting Information may be found in the online version of this article.

Correspondence to:

D. Bassett,
d.bassett@gns.cri.nz

Citation:

Bassett, D., Fujie, G., Kodaira, S., Arai, R., Yamamoto, Y., Henrys, S., et al. (2023). Heterogeneous crustal structure of the Hikurangi Plateau revealed by SHIRE seismic data: Origin and implications for plate boundary tectonics. *Geophysical Research Letters*, *50*, e2023GL105674. https://doi.org/10.1029/2023GL105674

Received 26 JUL 2023
Accepted 22 OCT 2023

Author Contributions:

Conceptualization: Shuichi Kodaira, Stuart Henrys, Harm van Avendonk, David Okaya, Kimi Mochizuki
Data curation: Gou Fujie, Katie Jacobs
Formal analysis: Dan Bassett, Gou Fujie
Funding acquisition: Shuichi Kodaira, Stuart Henrys, Harm van Avendonk, Nathan Bangs, David Okaya, Kimi Mochizuki

1. Introduction

The arrival of oceanic plateaux, large igneous provinces and oceanic ridges at active margins can have a major impact on the structure, configuration and deformation of plate boundaries, and in some cases have caused major, widespread changes in tectonic plate motions (Knesel et al., 2008; Shulgin et al., 2011; Wessel & Kroenke, 2000; Wood & Davy, 1994). Thickened oceanic crust increases the buoyancy and rigidity of the incoming plate, impacting the geometry of the subducting slab and promoting uplift, erosion and exhumation of the overriding plate (Arai et al., 2017; Shulgin et al., 2011; Tetreault & Buiter, 2012; Vogt & Gerya, 2014; Worthington et al., 2012). These factors may impact the magnitude of normal stresses across the subduction interface (e.g., Contreras-Reyes et al., 2019) and lateral crustal thickness variations have been linked to changes in both megathrust slip behavior (Kelleher & McCann, 1976; Shulgin et al., 2011) and stress-state in the subducting slab (Arai et al., 2017).

The Hikurangi Plateau is subducting along New Zealand's Hikurangi margin at a rate of ~20–60 mm/year (Figure 1) (Mortimer & Parkinson, 1996; Reyners et al., 2011; Wallace et al., 2004). The Plateau is thought to have formed between ~96 and 118 Ma as part of a larger Hikurangi-Manihiki-Ontong Java Plateau, which would represent the largest magmatic event preserved at Earth's surface (Coffin & Eldholm, 1994; Davidson et al., 2023; Hoernle et al., 2010; Taylor, 2006; Tejada et al., 2023; Timm et al., 2011). Rifting, followed by seafloor spreading at the Osbourn Trough separated the Hikurangi and Manihiki Plateaus, with the Hikurangi Plateau drifting south

Investigation: Dan Bassett, Gou Fujie, Shuichi Kodaira, Ryuta Arai, Yojiro Yamamoto, Dan Barker, Andrew Gase, Harm van Avendonk, Nathan Bangs, Hannu Seebeck, Brook Tozer, Katie Jacobs, Thomas Luckie, David Okaya, Kimi Mochizuki
Methodology: Dan Bassett, Gou Fujie
Project Administration: Shuichi Kodaira, Stuart Henrys, Harm van Avendonk, Nathan Bangs, David Okaya, Kimi Mochizuki
Supervision: Shuichi Kodaira, Stuart Henrys
Writing – original draft: Dan Bassett, Gou Fujie, Stuart Henrys, Andrew Gase, Hannu Seebeck
Writing – review & editing: Dan Bassett, Gou Fujie, Shuichi Kodaira, Ryuta Arai, Yojiro Yamamoto, Stuart Henrys, Dan Barker, Andrew Gase, Harm van Avendonk, Nathan Bangs, Hannu Seebeck, Brook Tozer, Katie Jacobs, Thomas Luckie, David Okaya, Kimi Mochizuki

before its collision and incipient subduction at the Gondwana margin, which has been linked to the cessation of subduction in this region (Billen & Stock, 2000; Davy et al., 2008a; Hoernle et al., 2020; Lonsdale, 1997; Riefstahl et al., 2020; Wood & Davy, 1994). Dredge samples and scientific drilling show the Plateau sequence consists predominantly of a 96–118 Ma tholeiitic basaltic basement (Hoernle et al., 2010) overlain by Cretaceous clastic sedimentary rocks and Late Cretaceous to Early Oligocene chalks and mudstones (Barnes et al., 2020; Davy et al., 2008b). Seamounts (52–99 Ma), of alkali basalt composition (Hoernle et al., 2010) and younger Cenozoic intraplate volcanoes (Timm et al., 2010) are prominent features of the Plateau (Barnes et al., 2010, 2018; Collot et al., 2001; Lewis et al., 1998), the subduction of which along the northern Hikurangi margin has been linked to the occurrence of tsunami earthquakes (Bell et al., 2014), shallow slow slip events, repeating earthquakes and tremor (Barker et al., 2018; Shaddox & Schwartz, 2019; Sun et al., 2020; Todd et al., 2018; Wallace et al., 2016).

In this study, we present a new 460 km long geophysical transect along the Hikurangi Plateau parallel and outboard of the active Hikurangi margin to resolve the distribution of seamounts and determine the crustal thickness, structure, and sediment cover sequence. We integrate regional data sets to provide new insights on Plateau structure and consider the impact of heterogeneous crustal structure on plate boundary deformation and megathrust slip behavior.

2. Marine Geophysical Data

2.1. Data Acquisition

Multichannel seismic reflection (MCS) and wide-angle seismic data were acquired by the R/V *Marcus G. Langseth* (Figure 2) as a part of the SHIRE Experiment (Bangs, 2018; Barker et al., 2019). The seismic source was a

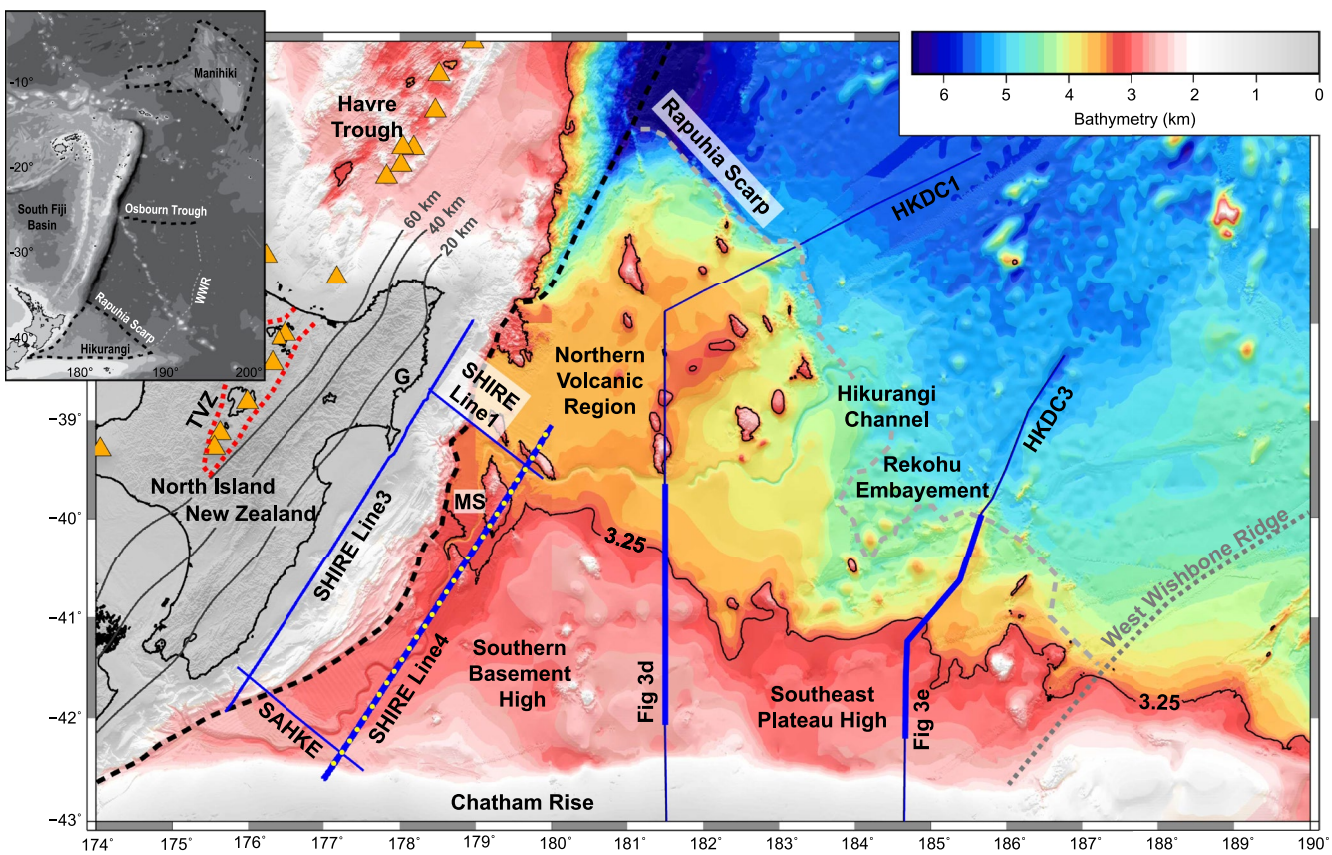

Figure 1. Tectonic settings and geophysical data. Hikurangi subduction zone, New Zealand. Thick blue lines show wide-angle seismic profiles collected during SHIRE. Yellow dots mark Ocean Bottom Seismometers. Thin blue lines mark HKDC1 and HKDC3 seismic reflection profiles, with thick sections marking the segments used for the construction of gravity models (Figures 3d and 3e). Orange triangles mark active volcanoes. Note the abrupt contrast in water-depth between the northern and southern Hikurangi Plateau. Inset shows regional tectonic setting. Annotation: G = Gisborne, TVZ = Taupo Volcanic Zone, WWR = West Wishbone Ridge. MS = Mahia Seamount.

tuned air-gun array (6,600 in^3, 13.1 MPa) towed at 9 m depth, with Line 4 first acquired using a 50 m shot spacing for the MCS data, followed by 200 m interval for wide-angle seismic data. MCS data were recorded by a 12.8 km long, 1,008 channel receiver array towed at 10 m depth. Wide-angle data were recorded using 30 Ocean Bottom Seismometers (OBSs) deployed at ∼15 km intervals by R/V *Tangaroa*.

2.2. Data Processing and Tomography

The MCS data processing sequence consisted of resampling to 4 ms, band-limited swell noise suppression (0–3 Hz), velocity analysis, surface-related multiple elimination, parabolic radon transform and amplitude recovery. Pre-stack time migration was applied to obtain the final seismic reflection section (Figure 2a).

Wide-angle seismic data were processed using a 4–20 Hz band-pass filter (Figure S1 in Supporting Information S1). From OBS receiver gathers, we picked 19,302 first-arrival travel-times associated with refractions through the crust (Pg) and mantle (Pn) of the Hikurangi Plateau, and 5,031 wide-angle reflections (PmP) from the base (Moho) of the Plateau. The OBS data quality is excellent, with first arrivals identified to >100 km offset on most instruments. Travel-time tomography was undertaken to construct a layered P-wave (Vp) seismic velocity model, simultaneously solving for seismic velocities of the crust and mantle, and the geometry of the Moho (Fujie et al., 2013, 2016). Seismic velocities were determined within a regular grid discretized 3.0 km horizontally and 0.25 km vertically. The Moho interface was modeled along nodes with 10 km spacing. Our final P-wave velocity model replicates observed travel-times with a root mean squared error of 44.7 ms (Figure S2 in Supporting Information S1).

Spatial resolution and uncertainties in seismic velocities were assessed using Monte Carlo and Checkerboard recovery approaches, the details and results of which are presented in Supporting Information S1.

3. Results

3.1. Hikurangi Plateau Structure From Seismic Reflection Data

Seismic reflection data along SHIRE Line 4 reveals five seamounts on the Hikurangi Plateau (Figure 2a). These seamounts are evenly distributed between north and south, typically rising 2–2.5 s (3–4 km) above the volcaniclastic sequences (HKB) interpreted to mark the top of the Hikurangi Plateau, with in-profile widths varying from 35 to 70 km. Despite subsurface similarity in seamount heights, their expression at the seafloor progressively increases from south to north. This is primarily due to reductions in sediment thickness, which decreases from >2.5 s TWTT (∼4.5 km) in the south to 1–1.5 s TWTT (∼1–2 km) in the north. The flanks of Mahia seamount appear interbedded within unit CL and stratigraphic inferences of young volcanism are consistent with the Pliocene age (3.2 ± 0.3 Ma) determined from ^{40}Ar/^{39}Ar dating of dredge samples (Timm et al., 2010).

The sediment cover between seamounts is interpreted following well-established seismic stratigraphic frameworks for the Hikurangi Plateau (Barnes et al., 2010, 2020; Davy et al., 2008a; Gase et al., 2022; Plaza-Faverola et al., 2012). Following this nomenclature and in order of increasing age, we interpret (a) a siliciclastic trench-fill sequence of hemipelagic turbidites (Unit TF—∼2.5 Ma—present), (b) a plateau cover sequence of nannofossil chalks interbedded with tephras and clays (Unit CL ∼32–>2.5 Ma), (c) a strongly reflective condensed sequence of chalk and shales (Sequence Y—70–32 Ma) underlain by a weakly reflective, possibly sandstone-rich, sequence of Late Cretaceous sediment (Unit MES—100–70 Ma). These sequences are all underlain by a highly reflective and widely distributed HKB unit (110 ± 10 Ma) associated with the volcaniclastic cover of the Hikurangi Plateau. The primary horizons separating these units are a regional erosional unconformity (Reflector 5B) that separates units TF and CL, and Reflector 7, which marks the top of Sequence Y and has been shown localize the initial formation of the décollement (i.e., megathrust) along the Hikurangi margin (Barnes et al., 2010; Plaza-Faverola et al., 2012). The base of MES is variably interpreted as underlain by HKB, or onlapping the flanks of seamounts.

At the southern end of the transect, seismic reflection data image the Mesozoic accretionary wedge of the Gondwana margin beneath the Chatham Rise (Model km 0–50—Figure 2a). Unit HKB is imaged underthrusting the accreted wedge, constraining the geometry of the relict Gondwana plate interface for ∼50 km. A change in seismic reflection character (dotted black line) is tentatively interpreted as the boundary between metasedimentary

10.1029/2023GL105674

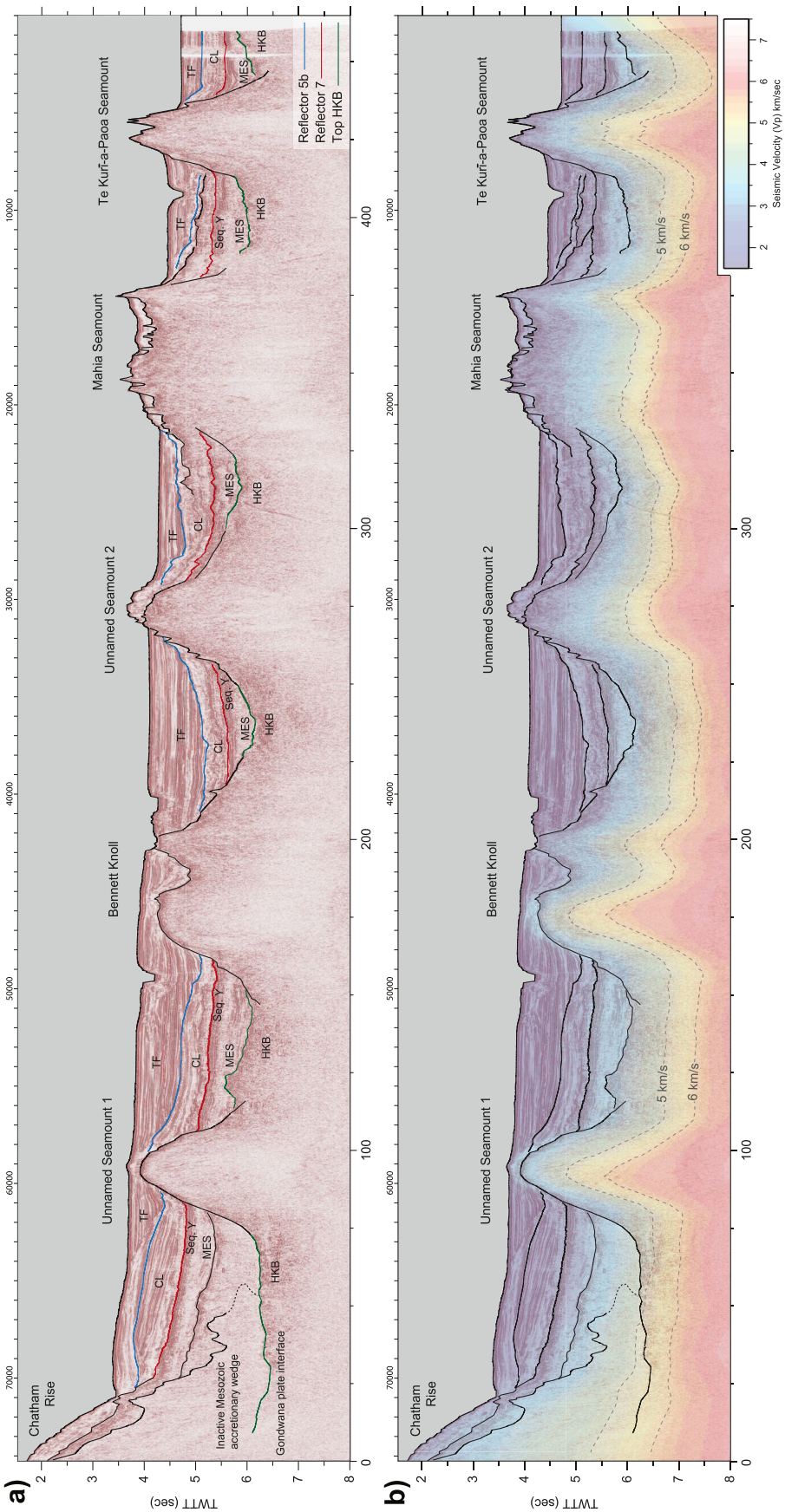

Figure 2. (a) Seismic reflection data along SHIRE Line 4. Colored lines mark reflectors separating trench-fill siliciclastics (TF), a pelagic plateau cover sequence (CL), condensed chalks and shales (Sequence Y), inferred Late Cretaceous siliciclastics (MES), and volcaniclastic cover of the Hikurangi Plateau (HKB) (Barnes et al., 2010; Davy et al., 2008b; Plaza-Faverola et al., 2012). (b) Seismic reflection section underlain by the wide-angle seismic velocity model. Note the heterogeneity in the internal structure of seamounts and the correspondence between seismic wavespeeds of 5–6 km/sec with the thickness of the highly reflective HKB sequence.

basement rocks that had undergone active accretion to the Gondwana margin (Mortimer et al., 2020), and sediments preserved within the trench or outer-wedge when Gondwana subduction terminated in the Early Cretaceous (Bland et al., 2015).

3.2. Hikurangi Plateau Structure From Wide-Angle Seismic Data

The seismic velocity structure of the Hikurangi Plateau derived from wide-angle seismic data is shown in Figure 3b. It is also shown underlying seismic reflection data in Figure 2b. Seismic velocities in the near-surface typically increase from 1.8 to 3.0 km/s through Stratigraphic Units TF and CL, before increasing further to 3.5 ± 0.2 at the base of MES (Figure 2b). Although we do not image a contiguous reflector marking the base of HKB, we note that spatial variability in the base of high-reflectivity associated with HKB is well correlated with seismic velocities of ~5.5–6 km/sec (Figure 2b). The upper 2–3 km of the Hikurangi Plateau is characterized by wavespeeds of 5.5–6.5 km/s and the lower crust has wavespeeds typically between 6.5 and 7.5 km/s.

The Moho of the Hikurangi Plateau is 18–19 km deep along the southern half of Line 4, but gradually shallows by 4 km between the northern flanks of Unnamed Seamount 2 (Model km 280—Figure 3b) and Mahia Seamount (Model km 380—Figure 3b), reaching a depth of 14 km at the northern end of the transect. These Moho depths are consistent with the results of margin-normal wide-angle seismic profiles traversing the Hikurangi Plateau in North (SHIRE Line 1) and South Hikurangi (SAHKE) respectively (Gase et al., 2021; Mochizuki et al., 2019). Excluding surficial volcaniclastics and taking 5.5 km/s to mark the top of the Hikurangi Plateau crust yields a crustal thickness of 10.5 ± 0.3 km south of Unnamed seamount 2 (Model km 280—Figures 3b) and 7 ± 0.5 km further north. Below the Moho, the mantle of the Hikurangi Plateau exhibits a heterogeneous velocity structure with wavespeeds typically ranging from 7.8 to 8.5 km/s. On average, seismic velocities are 0.2 km/s faster and appear more homogeneous in their distribution where the crust is thicker in the south, relative to the region of thinner crust further north.

The seismic velocity structure of seamounts is also heterogeneous. Unnamed Seamount 1 and Bennett Knoll are characterized by high-velocities, with wavespeeds exceeding 5 km/s within 2 km of the seamount crest and >6 km/s within the core of the seamount. Unnamed Seamount 2 and Mahia Seamount, by contrast, exhibit lower velocities with the top ~5 km of material <5 km/s. Te Kurī-a-Paoa Seamount exhibits an intermediate velocity gradient, with wavespeeds exceeding 5 km/s within 4 km of the seamount crest. Through the crust, Unnamed Seamounts 1 and 2, and Te Kurī-a-Paoa Seamount appear associated with reductions in seismic velocities in the upper crust, and we note that regions where the lower-crust does exhibit higher velocities appear to be between, rather than beneath, the seamounts imaged at shallow depth. High-resolution geophysical imaging of subducting and unsubducted seamounts offshore Gisborne show their internal structure to be heterogeneous with high-velocity and resistive cores embedded within a larger, lower-velocity and more conductive matrix (Arai et al., 2020; Chesley et al., 2021; Gase et al., 2021). We therefore suggest that differences in the seismic velocity structure of seamounts imaged along Line 4 reflect their three-dimensionality and position in relation to our 2D transect, rather than any overall differences in internal structure or composition. It is clear, for example, that our transect does not traverse the peak of Mahia seamount (Figure 1), which may explain the lower wavespeeds resolved.

3.3. Hikurangi Plateau Structure From Gravity Modeling

3.3.1. Western Plateau Structure Along SHIRE Line 4

Potential field data provide additional constraints on crustal structure, and we have conducted gravity modeling to (a) independently assess crustal structure in regions of lower or spatially heterogeneous ray-coverage; and (b) compare the crustal structure along SHIRE Line 4 with two MCS profiles father east on the Hikurangi Plateau (Figure 1). Our modeling strategy involves building an initial density model that preserves crustal structure where this is well determined, before adjusting less well constrained regions via perturbations to the density structure of the lower-crust, mantle and Moho geometry as required to replicate the observed Free-Air gravity anomaly. The construction of our starting model and the steps governing its subsequent refinement to replicate observed Free-Air gravity anomalies are detailed in Supporting Information S1 (Text S2).

The gravity model in Figure 3c shows the south-to-north increase in Free-Air gravity anomalies is highly consistent with the reduction in crustal thickness and Moho depth suggested by wide-angle data. Assuming the Moho

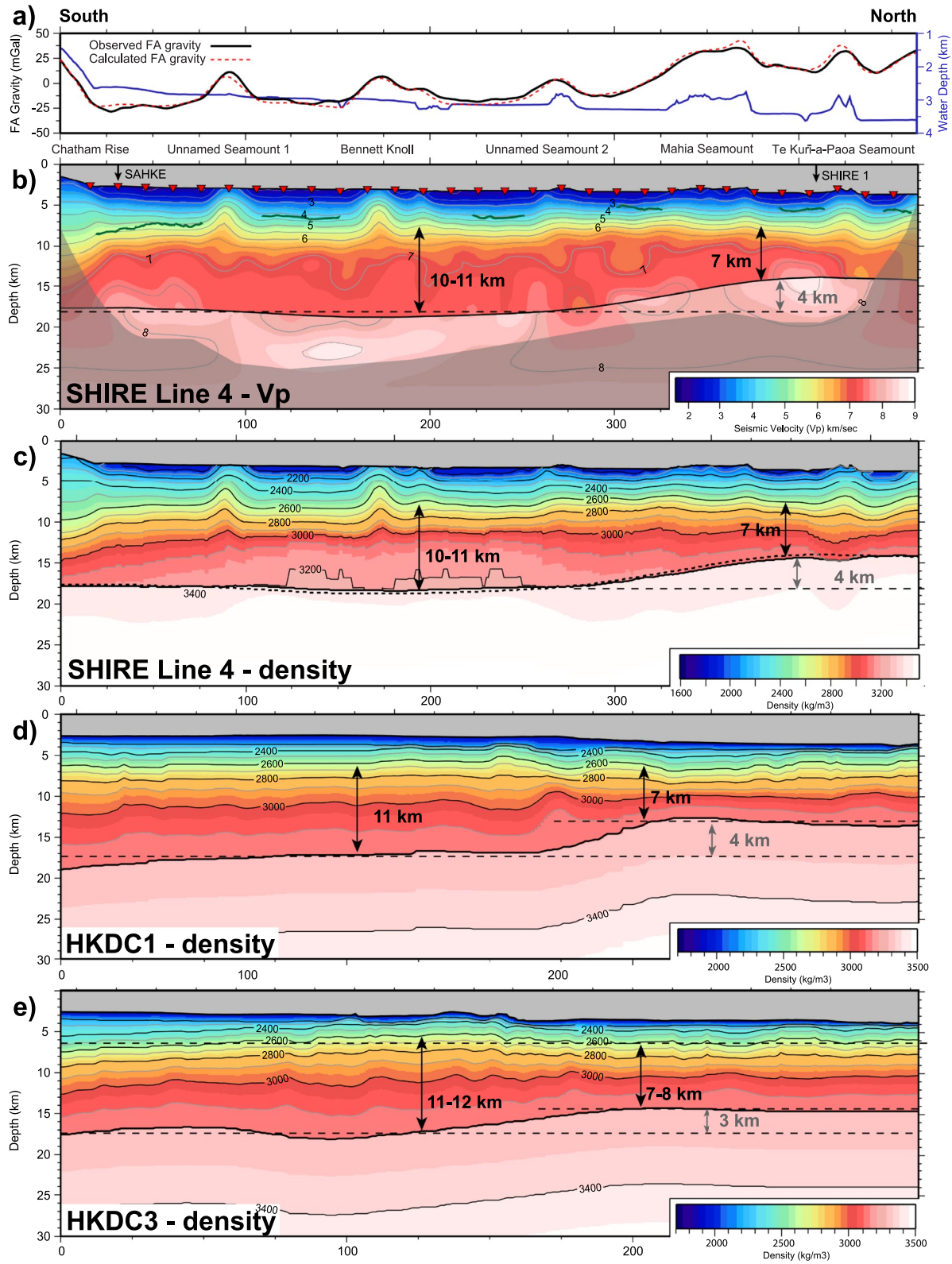

Figure 3. Hikurangi Plateau crustal structure (a) Bathymetry (blue) and observed (black) and calculated (red) Free-Air gravity anomalies along SHIRE Line4. (b) P-wave (V_P) seismic velocity along SHIRE Line 4. Red triangles mark Ocean Bottom Seismometers. Solid green line marks the top of Hikurangi Plateau volcaniclastic cover sequence (HKB). (c) Density models along SHIRE Line 4, (d) HKDC1 and (e) HKDC3.

geometry from wide-angle data is correct, then the reduction in seafloor bathymetry and crustal thickness must be accompanied by a south-to-north reduction in crustal and/or mantle densities. A reduction in mantle densities is consistent with average mantle velocities being 0.2 km/s slower beneath the region of thinner crust, relative to the southern portion of the model.

3.3.2. Central Plateau Structure Along HKDC MCS Lines

On the central Hikurangi Plateau, two additional seismic reflection lines (HKDC1 and HKDC3) cross the bathymetric step that broadly coincides with the reduction in crustal thickness along SHIRE Line 4 (Figure 1). These data were acquired in 2001 by the *Geco Resolution* (Davy et al., 2008a) and provide the requisite constraints on shallow crustal structure and sediment thickness for the construction of gravity models investigating crustal thickness variations farther east on the Hikurangi Plateau. HKDC1 and HKDC3 reveal the same stratigraphic sequences identified along SHIRE Line 4 (Figures S8 and S9 in Supporting Information S1) (Davy et al., 2008b). We have therefore used average 1-D velocity-depth functions determined along SHIRE Line 4 to build initial velocity and density models for HKDC lines, before following the same automated procedure of adjusting crustal densities and the geometry of the Moho to fit the short (<80 km) and long wavelength (>80 km) components of the Free-Air gravity anomaly respectively (Text S2 in Supporting Information S1).

These models show the depth of the Moho decreasing from south-to-north by 4 km along HKDC1 and ∼3 km along HKDC3 (Figures 3d and 3e). Taking 2600 kg/m^3 (equivalent to 5.5 km/s) to represent the top of the crust suggests a 3–4 km reduction in crustal thickness along both profiles. The magnitude of south-to-north reductions in both Moho depth and crustal thickness are similar to the results of SHIRE Line 4 and for all three models, the location of these reductions is well correlated with the SE-NW trending bathymetric step and the concomitant increase in water depth (Figure 1).

4. Discussion

Seismic velocity models derived from SHIRE wide-angle seismic transects and two seismically constrained gravity models further east on the Hikurangi Plateau (Figure 3) show that crustal thickness is 3–4 km thicker beneath the southern plateau highs (∼10–11 km), relative to the northern areas of the plateau (∼7–8 km). This contrast in crustal thickness may have existed prior to, or been generated during, the initial formation of the Ontong Java-Hikurangi-Manihiki Plateau. Alternatively, it may have developed during the subsequent rifting phase that accompanied plateau break-up.

In addition to constraining variability in crustal thickness, the regional Free-Air gravity field reveals structures that may inform both the origin of crustal thickness variability and its impact on contemporary tectonics. Along the Kermadec arc, the Free-Air gravity field of the incoming plate is dominated by a ∼500 km wide ∼40 mGal outer gravity-high that extends south of Osbourn Trough (Figures 4a and 4b). The dashed black-white lines show that the outer-gravity high is approximately parallel with iso-depth contours of the subducting slab (Hayes et al., 2018), with the similar spatial separation suggesting the radius of curvature of the Pacific Plate only changes gradually along the Kermadec arc. Figure 4a also shows the Kermadec gravity high extending through the Hikurangi Plateau to its juxtaposition with the Chatham Rise. One key difference, however, is that the strike of the gravity high is now oblique to the geometry of the subducting slab (Williams et al., 2013), suggesting a north-to-south increase in the radius of curvature of the Hikurangi Plateau. The obliquity and divergence of these structures is greatest within ∼100 km of the transition in crustal thickness (Figure 4a).

Global analyses of plate flexure at subduction zones show the broad wavelength of the outer-rise reflects the initial effective elastic thickness of the incoming plate, and that this strength must then reduce by as much as ∼40%–65% to replicate the steepness of the seaward wall of the trench (Garcia et al., 2019; Hunter & Watts, 2016). This strength reduction has been attributed to inelastic yielding (Wessel, 1992). As the width of outer-rise appears approximately constant (Figure 4a), we suggest thicker Hikurangi Plateau crust may be contributing to the shallower geometry of the subducting slab beneath the southern Hikurangi margin, potentially on account of both added buoyancy and by reducing the magnitude of the strength reduction due to inelastic yielding as the Plateau bends into the subduction zone.

Applying spectral averaging routines to remove the outer-gravity high reveals a contrast in structural fabric that may inform the origin of the transition in crustal thickness (Figure 4c). The northern plateau shows a strong

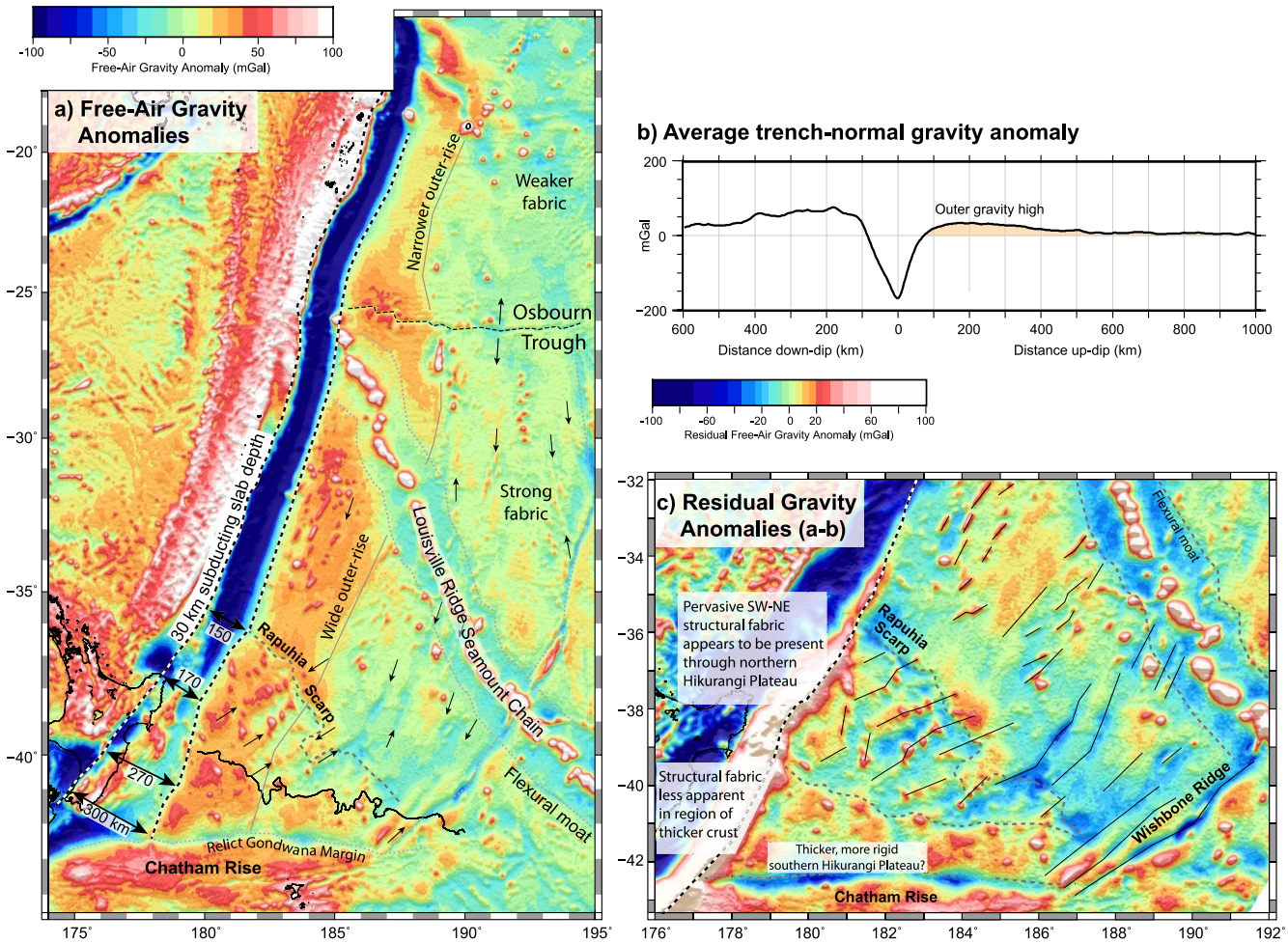

Figure 4. (a) Free-Air gravity anomalies along the Tonga-Kermadec-Hikurangi subduction zone (Sandwell et al., 2014). Dashed black-white lines approximate the trenchward limit of the outer-gravity high and the 30-km iso-depth contour for the subducting slab (Hayes et al., 2018; Williams et al., 2013).) Arrows highlight linear structures in the gravity field and alignments of seamounts. Spectral average of trench-normal gravity anomalies revealing the expression of the outer-gravity high. (c) Residual gravity anomalies after subtracting the spectral average of trench-normal gravity (Bassett & Watts, 2015a, 2015b). Note (1) the contrast in structure across the bathymetric scarp and (2) the similar orientation of gravity lineaments and seamounts through the northern Hikurangi Plateau with spreading related structure in the Pacific Ocean crust. In panel 4c, differences in gravity anomalies west of the outer-gravity high simply reflect differences in trench-depth and do not impact our interpretation of Hikurangi Plateau structure.

similarity to structures in the Pacific oceanic crust further north, with SW-NE striking lineaments identified in the residual gravity field, some of which can be tracked across Rapuhia Scarp (Figure 4c). We also interpret six SW-NE trending alignments of seamounts. The southern Hikurangi Plateau, by contrast, does not show a well-defined fabric and the West Wishbone Ridge is the only structure that can be traced with confidence across the bathymetric step (Barrett et al., 2018). The northeast-trending orientation of structures north of the bathymetric step is similar to the inferred direction of rifting between the Hikurangi and Manihiki Plateaux (Davy et al., 2008b). We suggest these structures may constrain the distribution of deformation associated with plateau breakup and that regional extension occurring over a similar area may have contributed to the contrast in crustal thickness resolved in this study. These alignments may be analogous to transverse alignments of seamounts observed at mid-ocean ridges and back-arc rifts, and may reflect transform structures that accommodate differences in the rates or orientation of rifting potentially providing larger and/or longer-lived structural pathways to be exploited by ascending melt.

The crust of the southern Hikurangi Plateau is similar in thickness (10–11 km) and velocity structure to the Western Manihiki Plateau and Tokelau Basin, and we note that variability in crustal thickness across the western Manihiki Plateau (Hochmuth et al., 2019), and south of the Chatham Rise (Riefstahl et al., 2020), has been

similarly attributed to extensional deformation. Juxtaposing the Hikurangi and Western Manihiki Plateaux before seafloor spreading implies asymmetric rifting where the northern Hikurangi Plateau has extended and thinned during rifting.

This model, which would impose additional coeval tectonic and long-lived thermal subsidence due to lithospheric extension across the northern Hikurangi Plateau may help explain bathymetric data showing the subsidence of guyots decreases almost linearly south of Rapuhia Scarp over a distance of ∼400 km (Hoernle et al., 2004). Spatial variability in deformation may also be expressed by differences in mantle seismic velocities. SHIRE wide-angle seismic surveys (Bassett et al., 2022; Gase et al., 2021; Mochizuki et al., 2019) and tomographic models (Eberhart-Phillips & Bannister, 2015) show that mantle velocities are systematically lower beneath the northern region of thinner crust. This may be due to differences in crustal thickness and curvature impacting the hydration and stress-state of the mantle (Arnulf et al., 2022; Fujie et al., 2023).

Collectively, we suggest observations of increased crustal thickness, a weaker structural fabric and deformation signature, and potentially differences in subsidence rates and mantle velocities are all consistent with the southern portion of the Hikurangi Plateau representing a more rigid and coherent lithosphere relative to the region further north. This rigidity and added buoyancy may contribute to spatial variability in short-term and long-term plate coupling and deformation associated with the Hikurangi subduction thrust. Present geodetic models show the plate interface is locked to ∼30 km depth along the southern Hikurangi margin (Wallace et al., 2012) and the thicker subducting crust, wider radius of curvature and shallower slab geometry (Williams et al., 2013) will contribute to the wide areal extent of this locked zone. Differences in crustal thickness and curvature will also influence the stress-state and permeability of the subducting plate, and may contribute to along-strike differences in the volume, chemistry and residence times of fluids derived from the subducting plate, the episodic release of which have been shown to play a key role in the generation of slow slip events along the north Hikurangi margin (Eberhart-Phillips et al., 2017; Mochizuki et al., 2021; Reyes et al., 2022; Warren-Smith et al., 2019). The contemporary stress state and long-term deformation of the upper plate may also have been impacted by variability in subducting crustal thickness (Nicol et al., 2007; Townend et al., 2012). Only the southern portion of the margin has rocks associated with basement terranes—composite Torlesse supergroup—uplifted and exposed in the coastal ranges (Heron, 2014), and we suggest higher rates of uplift and contraction in the southern North Island, may, in part, have been driven by north-south differences in the thickness and buoyancy of the Hikurangi Plateau (Jiao et al., 2017; Litchfield et al., 2007; Nicol et al., 2007; Nicol & Wallace, 2007).

Data Availability Statement

Raw and processed marine multi-channel seismic (MCS) data used in this study are available through Bangs et al. (2017). Ocean Bottom Seismograph data are available from GNS Science., 2017 and the JAMSTEC Seismic Survey Database (Barker, 2017).

Acknowledgments
This study was financially supported by JAMSTEC, by U.S National Science Foundation Grants: 1658010, 1657480, and 1615815, by the MBIE Endeavor Grant: Diagnosing peril posed by the Hikurangi subduction zone (contract C05X1605), and by public research funding from the Government of New Zealand Strategic Science Investment Fund to GNS Science (contract C05X1702). We thank the captain and crew of the *R/V M.G. Langseth* (MGL1708) and *R/V Tangaroa* (TAN1710). This manuscript has benefited from discussions with Bryan Davy, Christine Chesley, and G. T. Grey. We thank Lucy Flesh for editorial handling, and Christian Timm and an anomymous reviewer for constructive comments that have improved the manuscript. Figures were constructed using the Generic Mapping Tools (Wessel et al., 2019; Wessel & Smith, 1991).

References

Arai, R., Kodaira, S., Henrys, S., Bangs, N., Obana, K., Fujie, G., et al. (2020). Three-dimensional P wave velocity structure of the northern Hikurangi margin from the NZ3D experiment: Evidence for fault-bound anisotropy. *Journal of Geophysical Research: Solid Earth*, *125*(12), e2020JB020433. https://doi.org/10.1029/2020jb020433

Arai, R., Kodaira, S., Yamada, T., Takahashi, T., Miura, S., Kaneda, Y., et al. (2017). Subduction of thick oceanic plateau and high-angle normal-fault earthquakes intersecting the slab. *Geophysical Research Letters*, *44*(12), 6109–6115. https://doi.org/10.1002/2017gl073789

Arnulf, A. F., Bassett, D., Harding, A. J., Kodaira, S., Nakanishi, A., & Moore, G. (2022). Upper-plate controls on subduction zone geometry, hydration and earthquake behaviour. *Nature Geoscience*, *15*(2), 143–148. https://doi.org/10.1038/s41561-021-00879-x

Bangs, N. (2018). SHIRE project cruise report. In *Seismogenesis at Hikurangi integrated research experiment. November 1–December 7, 2017.89*. University of Texas Institute of Geophysics.

Bangs, N., Arnulf, A., van Avendonk, H., Saffer, D., Proctor, W., Okaya, D., et al. (2017). Project SHIRE: Seismogenesis at Hikurangi integrated research experiment [Dataset]. Lamont Academic Seismic Portal. https://doi.org/10.7284/907693

Barker, D. H. N. (2017). TAN1710 – Deployment and recovery of Ocean Bottom Seismometers during the sesimogenesis at Hikurangi integrated research experiment [Dataset]. JAMSTEC Seismic Survey Database. Retrieved from http://www.jamstec.go.jp/obsmcs_db/e/survey/data_area.html?cruise=TAN1710

Barker, D. H. N., Henrys, S., Caratori Tontini, F., Barnes, M., Bassett, D., Todd, E., & Wallace, L. (2018). Geophysical constraints on the relationship between seamount subduction, slow slip and tremor at the north Hikurangi subduction zone, New Zealand. *Geophysical Research Letters*, *45*(23), 12804–812813. https://doi.org/10.1029/2018gl080259

Barker, D. H. N., Van Avendonk, H., Fujie, G., & GNS Science (2019). Seismogenesis at Hikurangi integrated research experiment (SHIRE) report of RV Tangaroa cruise TAN1710, 23 Oct-20 Nov 2017, lower Hutt, N.Z., GNS Science. GNS Science report, 2019/01 (p. 22). + 23 appendices p.

Barnes, M., Ghisetti, F. C., Ellis, S., & Morgan, J. K. (2018). The role of protothrusts in frontal accretion and accommodation of plate convergence, Hikurangi subduction margin. *New Zealand: Geosphere*, *14*(2), 440–468. https://doi.org/10.1130/ges01552.1

Barnes, M., Lamarche, G., Bialas, J., Henrys, S., Pecher, I., Netzeband, G. L., et al. (2010). Tectonic and geological framework for gas hydrates and cold seeps on the Hikurangi subduction margin. *New Zealand: Marine Geology*, *272*(1–4), 26–48. https://doi.org/10.1016/j.margeo.2009.03.012

Barnes, M., Wallace, L. M., Saffer, D. M., Bell, R. E., Underwood, M. B., Fagereng, A., et al. (2020). Slow slip source characterized by lithological and geometric heterogeneity. *Science Advances*, *6*(13), eaay3314. https://doi.org/10.1126/sciadv.aay3314

Barrett, R. S., Davy, B., Stern, T., & Gohl, K. (2018). The strike-slip west wishbone ridge and the eastern margin of the Hikurangi Plateau. *Geochemistry, Geophysics, Geosystems*, *19*(4), 1199–1216. https://doi.org/10.1002/2017gc007372

Bassett, D., Arnulf, A., Henrys, S., Barker, D., van Avendonk, H., Bangs, N., et al. (2022). Crustal structure of the Hikurangi margin from SHIRE seismic data and the relationship between forearc structure and shallow megathrust slip behavior. *Geophysical Research Letters*, *49*(2), e2021GL096960. https://doi.org/10.1029/2021gl096960

Bassett, D., & Watts, A. B. (2015a). Gravity anomalies, crustal structure, and seismicity at subduction zones: 1. Seafloor roughness and subducting relief. *Geochemistry, Geophysics, Geosystems*, *16*(5), 32–1540. https://doi.org/10.1002/2014gc005684

Bassett, D., & Watts, A. B. (2015b). Gravity anomalies, crustal structure, and seismicity at subduction zones: 2. Interrelationships between fore-arc structure and seismogenic behavior. *Geochemistry, Geophysics, Geosystems*, *16*(5), 36–1576. https://doi.org/10.1002/2014gc005685

Bell, R., Holden, C., Power, W., Wang, X., & Downes, G. (2014). Hikurangi margin tsunami earthquake generated by slow seismic rupture over a subducted seamount. *Earth and Planetary Science Letters*, *397*, 1–9. https://doi.org/10.1016/j.epsl.2014.04.005

Billen, M. I., & Stock, J. (2000). Morphology and origin of the Osbourn Trough. *Journal of Geophysical Research, B, Solid Earth and Planets*, *105*(6), 13481–413489. https://doi.org/10.1029/2000jb900035

Bland, K. J., Uruski, C. I., & Isaac, M. J. (2015). Pegasus Basin, eastern New Zealand: A stratigraphic record of subsidence and subduction, ancient and modern. *New Zealand Journal of Geology and Geophysics*, *58*(4), 319–343. https://doi.org/10.1080/00288306.2015.1076862

Chesley, C., Naif, S., Key, K., & Bassett, D. (2021). Fluid-rich subducting topography generates anomalous forearc porosity. *Nature*, *595*(7866), 255–260. https://doi.org/10.1038/s41586-021-03619-8

Coffin, M. F., & Eldholm, O. (1994). Large igneous provinces: Crustal structure, dimensions, and external consequences. *Reviews of Geophysics*, *32*(1), 1–36. https://doi.org/10.1029/93rg02508

Collot, J. Y., Lewis, K., Lamarche, G., & Lallemand, S. (2001). The giant Ruatoria debris avalanche on the northern Hikurangi margin, New Zealand: Result of oblique seamount subduction. *Journal of Geophysical Research*, *106*(B9), 19271–19297. https://doi.org/10.1029/2001jb900004

Contreras-Reyes, E., Muñoz-Linford, P., Cortés-Rivas, V., Bello-González, J., Ruiz, J., & Krabbenhoeft, A. (2019). Structure of the collision zone between the Nazca ridge and the Peruvian convergent margin: Geodynamic and seismotectonic implications. *Tectonics*, *38*(9), 3416–3435. https://doi.org/10.1029/2019tc005637

Davidson, C., Koppers, A. A., Sano, T., & Hanyu, T. (2023). A younger and protracted emplacement of the Ontong Java Plateau. *Science*, *380*(6650), 1185–1188. https://doi.org/10.1126/science.ade8666

Davy, B., Hoernle, K., & Werner, R. (2008a). Hikurangi Plateau: Crustal structure, rifted formation, and Gondwana subduction history. *Geochemistry, Geophysics, Geosystems*, *9*(7), Q07004. https://doi.org/10.01029/02007GC001855

Davy, B. R., Hoernle, K., & Werner, R. (2008b). The Hikurangi Plateau—Crustal structure, rifted formation and Gonwana subduction history. *Geochemistry, Geophysics, Geosystems*, *9*(7), Q07004. https://doi.org/10.1029/2007gc001855

Eberhart-Phillips, D., & Bannister, S. (2015). 3-D imaging of the northern Hikurangi subduction zone, New Zealand: Variations in subducted sediment, slab fluids and slow slip. *Geophysical Journal International*, *201*(2), 838–855. https://doi.org/10.1093/gji/ggv057

Eberhart-Phillips, D., Bannister, S., & Reyners, M. (2017). Deciphering the 3-D distribution of fluid along the shallow Hikurangi subduction zone using P-and S-wave attenuation. *Geophysical Journal International*, *211*(2), 1032–1045. https://doi.org/10.1093/gji/ggx348

Fujie, G., Kodaira, S., Obana, K., Yamamoto, Y., Isse, T., Yamada, T., et al. (2023). The nature of the Pacific plate as subduction inputs to the northeastern Japan arc and its implication for subduction zone processes. *Progress in Earth and Planetary Science*, *10*(1), 50. https://doi.org/10.1186/s40645-023-00578-8

Fujie, G., Kodaira, S., Sato, T., & Takahashi, T. (2016). Along-trench variations in the seismic structure of the incoming Pacific plate at the outer rise of the northern Japan Trench. *Geophysical Research Letters*, *43*(2), 666–673. https://doi.org/10.1002/2015gl067363

Fujie, G., Kodaira, S., Yamashita, M., Sato, T., Takahashi, T., & Takahashi, N. (2013). Systematic changes in the incoming plate structure at the Kuril trench. *Geophysical Research Letters*, *40*(1), 88–93. https://doi.org/10.1029/2012gl054340

Garcia, E. S. M., Sandwell, D. T., & Bassett, D. (2019). Outer trench slope flexure and faulting at Pacific basin subduction zones. *Geophysical Journal International*, *218*(1), 708–728. https://doi.org/10.1093/gji/ggz155

Gase, A. C., Bangs, N., Van Avendonk, H. J., Bassett, D., Henrys, S., Barker, D., et al. (2021). Crustal structure of the northern Hikurangi margin, New Zealand: Variable accretion and upper plate strength influenced by rough subduction. *Journal of Geophysical Research: Solid Earth*, *126*, e2020JB021176. https://doi.org/10.1029/2020JB021176

Gase, A. C., Bangs, N. L., Van Avendonk, H. J., Bassett, D., & Henrys, S. A. (2022). Hikurangi megathrust slip behavior influenced by lateral variability in sediment subduction: Geology.

Hayes, G. P., Moore, G. L., Portner, D. E., Hearne, M., Flamme, H., Furtney, M., & Smoczyk, G. M. (2018). Slab2, a comprehensive subduction zone geometry model. *Science*, *362*(6410), 58–61. https://doi.org/10.1126/science.aat4723

Heron, D. (2014). Geological map of New Zealand: Institute of geological and Nuclear sciences 1: 250,000 geological map 1: Lower Hutt: New Zealand, GNS science, scale, 1, 250,000, 1.

Hochmuth, K., Gohl, K., Uenzelmann-Neben, G., & Werner, R. (2019). Multiphase magmatic and tectonic evolution of a large igneous province-Evidence from the crustal structure of the Manihiki Plateau, western Pacific. *Tectonophysics*, *750*, 434–457. https://doi.org/10.1016/j.tecto.2018.11.014

Hoernle, K., Hauff, F., Van den Bogaard, P., Werner, R., Mortimer, N., Geldmacher, J., et al. (2010). Age and geochemistry of volcanic rocks from the Hikurangi and Manihiki oceanic Plateaus. *Geochimica et Cosmochimica Acta*, *74*(24), 7196–7219. https://doi.org/10.1016/j.gca.2010.09.030

Hoernle, K., Hauff, F., Werner, R., & Mortimer, N. (2004). New insights into the origin and evolution of the Hikurangi oceanic plateau: Eos. *Transactions - American Geophysical Union*, *85*(41), 401–408. https://doi.org/10.1029/2004eo410001

Hoernle, K., Timm, C., Hauff, F., Tappenden, V., Werner, R., Jolis, E., et al. (2020). Late Cretaceous (99-69 Ma) basaltic intraplate volcanism on and around Zealandia: Tracing upper mantle geodynamics from Hikurangi Plateau collision to Gondwana breakup and beyond. *Earth and Planetary Science Letters*, *529*, 115864. https://doi.org/10.1016/j.epsl.2019.115864

Hunter, J., & Watts, A. (2016). Gravity anomalies, flexure and mantle rheology seaward of circum-Pacific trenches. *Geophysical Journal International*, *207*(1), 288–316. https://doi.org/10.1093/gji/ggw275

Jiao, R., Herman, F., & Seward, D. (2017). Late Cenozoic exhumation model of New Zealand: Impacts from tectonics and climate. *Earth-Science Reviews*, *166*, 286–298. https://doi.org/10.1016/j.earscirev.2017.01.003

Kelleher, J., & McCann, W. (1976). Buoyant zones, great earthquakes, and unstable boundaries of subduction. *Journal of Geophysical Research*, *81*(26), 4885–4896. https://doi.org/10.1029/jb081i026p04885

Knesel, K. M., Cohen, B. E., Vasconcelos, M., & Thiede, D. S. (2008). Rapid change in drift of the Australian plate records collision with Ontong Java plateau. *Nature*, *454*(7205), 754–757. https://doi.org/10.1038/nature07138

Lewis, K. B., Collot, J.-Y., & Lallemand, S. E. (1998). The dammed Hikurangi trough: A channel-fed trench blocked by subducting seamounts and their wake avalanches (New Zealand-France GeodyNZ Project). *Basin Research*, *10*(4), 441–468. https://doi.org/10.1046/j.1365-2117.1998.00080.x

Litchfield, N., Ellis, S., Berryman, K., & Nicol, A. (2007). Insights into subduction-related uplift along the Hikurangi Margin, New Zealand, using numerical modeling. *Journal of Geophysical Research*, *112*(F2), F02021. https://doi.org/10.1029/2006JF000535

Lonsdale, F. (1997). An incomplete geologic history of the southwest Pacific basin—Hpothesis for Cretaceous rifting of east Gondwana caused by subducted slab capture. *Geological Society of America, Abstracts With Programs*, *5*, 4574.

Mochizuki, K., Henrys, S., Haijima, D., Warren-Smith, E., & Fry, B. (2021). Seismicity and velocity structure in the vicinity of repeating slow slip earthquakes, northern Hikurangi subduction zone, New Zealand. *Earth and Planetary Science Letters*, *563*, 116887. https://doi.org/10.1016/j.epsl.2021.116887

Mochizuki, K., Sutherland, R., Henrys, S., Bassett, D., Van Avendonk, H., Arai, R., et al. (2019). Recycling of depleted continental mantle by subduction and plumes at the Hikurangi Plateau large igneous province. *Southwestern Pacific Ocean: Geology*, *47*(8), 795–798. https://doi.org/10.1130/g46250.1

Mortimer, N., Campbell, H. J., & Moerhuis, N. (2020). Chatham schist: New Zealand. *Journal of Geology and Geophysics*, *63*(2), 237–249. https://doi.org/10.1080/00288306.2019.1662817

Mortimer, N., & Parkinson, D. (1996). Hikurangi Plateau: A cretaceous large igneous province in the southwest Pacific ocean. *Journal of Geophysical Research*, *101*(B1), 687–696. https://doi.org/10.1029/95jb03037

Nicol, A., Mazengarb, C., Chanier, F., Rait, G., Uruski, C. I., & Wallace, L. M. (2007). Tectonic evolution of the active Hikurangi subduction margin. *New Zealand, Since the Oligocene: Tectonics*, *26*(4), TC4002. https://doi.org/10.1029/2006TC002090

Nicol, A., & Wallace, L. M. (2007). Temporal stability of deformation rates: Comparison of geological and geodetic observations, Hikurangi subduction margin. *New Zealand: Earth and Planetary Science Letters*, *258*(3/4), 397–413. https://doi.org/10.1016/j.epsl.2007.1003.1039

Plaza-Faverola, A., Klaeschen, D., Barnes, P., Pecher, I., Henrys, S., & Mountjoy, J. (2012). Evolution of fluid expulsion and concentrated hydrate zones across the southern Hikurangi subduction margin, New Zealand: An analysis from depth migrated seismic data. *Geochemistry, Geophysics, Geosystems*, *13*, 8. https://doi.org/10.1029/2012gc004228

Reyes, A. G., Ellis, S. M., Christenson, B. W., & Henrys, S. (2022). Fluid flowrates and compositions and water–rock interaction in the Hikurangi margin forearc. *New Zealand: Chemical Geology*, *614*, 121169. https://doi.org/10.1016/j.chemgeo.2022.121169

Reyners, M., Eberhart-Phillips, D., & Bannister, S. (2011). Tracking repeated subduction of the Hikurangi Plateau beneath New Zealand. *Earth and Planetary Science Letters*, *311*(1), 165–171. https://doi.org/10.1016/j.epsl.2011.09.011

Riefstahl, F., Gohl, K., Davy, B., Hoernle, K., Mortimer, N., Timm, C., et al. (2020). Cretaceous intracontinental rifting at the southern Chatham Rise margin and initialisation of seafloor spreading between Zealandia and Antarctica. *Tectonophysics*, *776*, 228298. https://doi.org/10.1016/j.tecto.2019.228298

Sandwell, D. T., Müller, D. T., Smith, W. H. F., Garcia, E., & Francis, R. (2014). New global marine gravity from CryoSat-2 and jacon-1 reveals buried tectonic structure. *Science*, *346*, 6205.

Shaddox, H. R., & Schwartz, S. Y. (2019). Subducted seamount diverts shallow slow slip to the forearc of the northern Hikurangi subduction zone. *New Zealand: Geology*, *47*(5), 415–418. https://doi.org/10.1130/g45810.1

Shulgin, A., Kopp, H., Mueller, C., Planert, L., Lueschen, E., Flueh, E., & Djajadihardja, Y. (2011). Structural architecture of oceanic plateau subduction offshore Eastern Java and the potential implications for geohazards. *Geophysical Journal International*, *184*(1), 12–28. https://doi.org/10.1111/j.1365-246x.2010.04834.x

Sun, T., Saffer, D., & Ellis, S. (2020). Mechanical and hydrological effects of seamount subduction on megathrust stress and slip. *Nature Geoscience*, *13*(3), 249–255. https://doi.org/10.1038/s41561-020-0542-0

Taylor, B. (2006). The single largest oceanic plateau: Ontong Java–Manihiki–Hikurangi. *Earth and Planetary Science Letters*, *241*(3), 372–380. https://doi.org/10.1016/j.epsl.2005.11.049

Tejada, M., Sano, T., Hanyu, T., Koppers, A., Nakanishi, M., Miyazaki, T., et al. (2023). New evidence for the Ontong Java Nui hypothesis. *Scientific Reports*, *13*(1), 8486. https://doi.org/10.1038/s41598-023-33724-9

Tetreault, J. á., & Buiter, S. (2012). Geodynamic models of terrane accretion: Testing the fate of island arcs, oceanic plateaus, and continental fragments in subduction zones. *Journal of Geophysical Research*, *117*(B8), B08403. https://doi.org/10.1029/2012jb009316

Timm, C., Hoernle, K., Werner, R., Hauff, F., van den Bogaard, P., Michael, P., et al. (2011). Age and geochemistry of the oceanic Manihiki Plateau, SW Pacific: New evidence for a plume origin. *Earth and Planetary Science Letters*, *304*(1–2), 135–146. https://doi.org/10.1016/j.epsl.2011.01.025

Timm, C., Hoernle, K., Werner, R., Hauff, F., van den Bogaard, P., White, J., et al. (2010). Temporal and geochemical evolution of the Cenozoic intraplate volcanism of Zealandia. *Earth-Science Reviews*, *98*(1–2), 38–64. https://doi.org/10.1016/j.earscirev.2009.10.002

Todd, E., Schwatz, S., Williams, C., Sheehan, A., Mochizuki, K., Henrys, S., et al. (2018). Shallow slow slip and tremor associated with seamount subduction offshore Gisborne, Hikurangi margin. *New Zealand Journal of Geophysical Research*, *6*(3), https://doi.org/10.1126/sciadv.aay5786

Townend, J., Sherburn, S., Arnold, R., Boese, C., & Woods, L. (2012). Three-dimensional variations in present-day tectonic stress along the Australia–Pacific plate boundary in New Zealand. *Earth and Planetary Science Letters*, *353*, 47–59. https://doi.org/10.1016/j.epsl.2012.08.003

Vogt, K., & Gerya, T. V. (2014). From oceanic plateaus to allochthonous terranes: Numerical modelling. *Gondwana Research*, *25*(2), 494–508. https://doi.org/10.1016/j.gr.2012.11.002

Wallace, L., Barnes, P., Beavan, J., Van Dissen, R., Litchfield, N., Mountjoy, J., et al. (2012). The kinematics of a transition from subduction to strike-slip: An example from the central New Zealand plate boundary. *Journal of Geophysical Research*, *117*(B2), B02405. https://doi.org/10.1029/2011jb008640

Wallace, L. M., Beavan, J., McCaffrey, R., & Darby, D. (2004). Subduction zone coupling and tectonic block rotations in the North Island, New Zealand. *Journal of Geophysical Research*, *109*(B12), B12406. https://doi.org/10.1029/2004JB003241

Wallace, L. M., Webb, S. C., Ito, Y., Mochizuki, K., Hino, R., Henrys, S. A., et al. (2016). Slow slip near the trench at the Hikurangi subduction zone, New Zealand. *Science*, *352*(6286), 701–704. https://doi.org/10.1126/science.aaf2349

Warren-Smith, E., Fry, B., Wallace, L., Chon, E., Henrys, S., Sheehan, A., et al. (2019). Episodic stress and fluid pressure cycling in subducting oceanic crust during slow slip. *Nature Geoscience*, *12*(6), 475–481. https://doi.org/10.1038/s41561-019-0367-x

Wessel, P. (1992). Thermal stresses and the bimodal distribution of elastic thickness estimates of the oceanic lithosphere. *Journal of Geophysical Research*, *97*(B10), 14177–14193. https://doi.org/10.1029/92jb01224

Wessel, P., & Kroenke, L. W. (2000). Ontong Java Plateau and late Neogene changes in Pacific plate motion. *Journal of Geophysical Research*, *105*(B12), 28255–28277. https://doi.org/10.1029/2000jb900290

Wessel, P., Luis, J., Uieda, L., Scharroo, R., Wobbe, F., Smith, W., & Tian, D. (2019). The generic mapping tools version 6. *Geochemistry, Geophysics, Geosystems*, *20*(11), 5556–5564. https://doi.org/10.1029/2019gc008515

Wessel, P., & Smith, W. H. (1991). Free software helps map and display data: Eos. *Transactions - American Geophysical Union*, *72*(41), 441–446. https://doi.org/10.1029/90eo00319

Williams, C. A., Eberhart-Phillips, D., Bannister, S., Barker, D. H., Henrys, S., Reyners, M., & Sutherland, R. (2013). Revised interface geometry for the Hikurangi subduction zone, New Zealand. *Seismological Research Letters*, *84*(6), 1066–1073. https://doi.org/10.1785/0220130035

Wood, R., & Davy, B. (1994). The Hikurangi Plateau. *Marine Geology*, *118*(1–2), 153–173. https://doi.org/10.1016/0025-3227(94)90118-x

Worthington, L. L., Van Avendonk, H. J., Gulick, S. P., Christeson, G. L., & Pavlis, T. L. (2012). Crustal structure of the Yakutat terrane and the evolution of subduction and collision in southern Alaska. *Journal of Geophysical Research*, *117*(B1), B01102. https://doi.org/10.1029/2011jb008493

References From the Supporting Information

Bott, M. (1965). The deep structure of the northern Irish Sea-a problem of crustal dynamics. *Colston Papers*, *17*, 179–204.

Christensen, N. I., & Mooney, W. D. (1995). Seismic velocity structure and composition of the continental crust: A global view. *Journal of Geophysical Research*, *100*(B6), 9761–9788. https://doi.org/10.1029/95jb00259

GNS Science. (2017). Seismogenesis at Hikurangi integrated research experiment (SHIRE) offshre data [Dataset]. GNS Science Dataset Catalogue. https://doi.org/10.21420/TQ67-8F60

Nafe, J. E., & Drake, C. L. (1961). *Physical properties of marine sediments*. Lamont Geological Observatory Palisadesny.